

# Communications

## The Folded Horn Antenna

Everett G. Farr, Leland H. Bowen, Carl E. Baum, and  
William D. Prather

**Abstract**—Antennas for radiating high-power mesoband (medium-bandwidth) electromagnetic signals are critical to the mission of upsetting electronics at a distance. When operated at frequencies of a few hundred megahertz, RF weapons require highly efficient antennas that can fit into a small volume. Most of the existing antennas, such as pyramidal horns, are too large to fit onto certain platforms of interest. To address this challenge, we investigate the folded horn, which has aperture dimensions of  $0.5 \times 2$  wavelengths, and a depth of 1.5–2 wavelengths. This antenna has a nearly focused aperture field, due to a parabolic fold in the H-plane. We report here on the fabrication and testing of the first folded horn, operating at 3 GHz. After a number of iterations, we obtained a realized gain of at least 10 dBi over 3–5 GHz, an aperture efficiency of 80%, and a return loss below  $-10$  dB over 2.8–3.35 GHz. This design could be adapted to high voltages, and it could work well in a 2-antenna array, with two antennas positioned back-to-back, driven by a differential source.

**Index Terms**—Antenna gain, antenna radiation patterns, horn antennas, weapons.

### I. INTRODUCTION

We introduce here a new antenna, the folded horn. This antenna was first proposed by C. E. Baum for radiating high-power mesoband (medium-bandwidth) signals from a very compact package with high efficiency and moderate gain [1]. It was intended to operate at a frequency of a few hundred megahertz, for the application of upsetting electronics at a distance. In this paper we provide the first experimental results for the folded horn.

The advantage of a folded horn over a pyramidal horn is that it has no dimension larger than 2 wavelengths. The requirement to keep the antenna size small becomes apparent at lower frequencies. For example, at 200 MHz, where the wavelength is 1.5 m, a folded horn with aperture dimensions of  $0.5 \times 2\lambda$  and depth of  $1.7\lambda$  has a size of  $0.75 \times 3 \times 2.6$  m. An antenna of this size can fit onto the bed of a truck while looking sideways. However, for example, a pyramidal horn would not fit into such a limited space at this frequency.

In this paper, we build and test the first prototype low-power folded horn, operating at a nominal operating frequency of 3 GHz. We tried several iterations, resulting in a design that satisfies our requirements over 3–5 GHz. We also describe alternative configurations, and we suggest further improvements that could result in either improved performance or a more compact size. We begin now with a description of the folded horn.

Manuscript received January 14, 2007; revised June 13, 2007. This work was supported by the Air Force Research Laboratory, Directed Energy Directorate.

E. G. Farr and L. H. Bowen are with Farr Research, Inc., Albuquerque, NM 87123 USA (e-mail: efarr@farr-research.com).

C. E. Baum is with the University of New Mexico, Albuquerque, NM 87131 USA.

W. D. Prather is with the Air Force Research Laboratory, Directed Energy Directorate, Kirtland AFB, NM 87117 USA.

Color versions of one or more of the figures in this paper are available online at <http://ieeexplore.ieee.org>.

Digital Object Identifier 10.1109/TAP.2007.908854

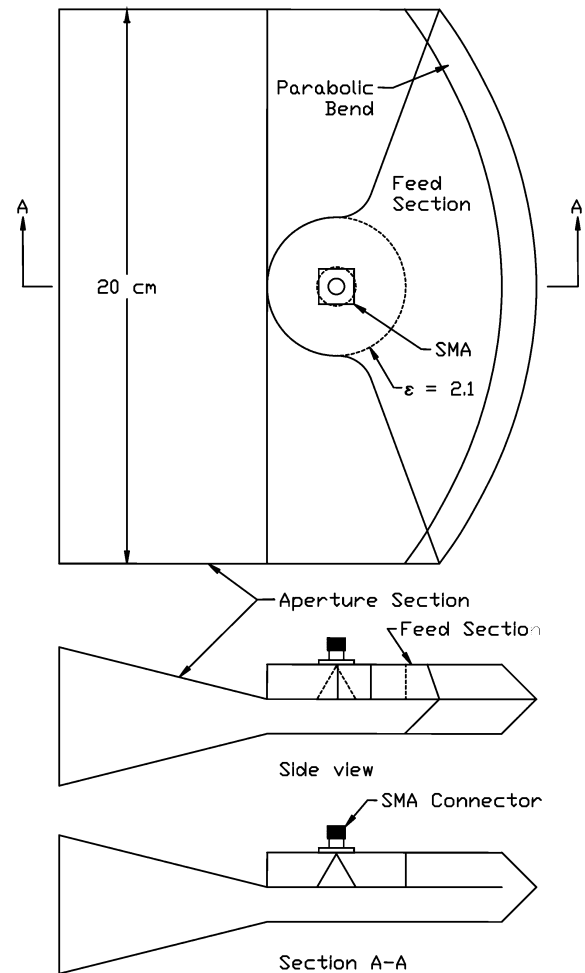


Fig. 1. Folded horn, model FH-1E.

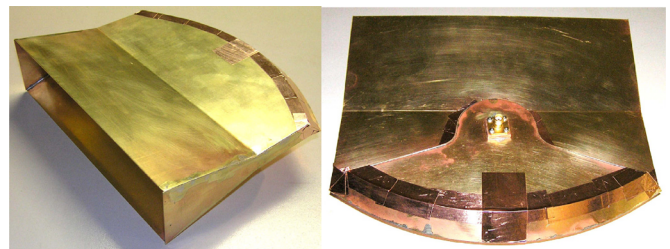


Fig. 2. Top and bottom view of the FH-1E.

### II. FOLDED HORN DESIGN AND ANALYSIS

We describe here the basic design and operation of the folded horn, and we provide an analysis of its performance. A sketch of the folded horn is shown in Fig. 1, and photos are shown in Fig. 2. This device consists of three parts: the feed section, the parabolic bend, and the aperture section. At its design frequency of 3 GHz, this antenna has an aperture of  $0.5 \times 2\lambda$ , and a depth of  $1.75\lambda$ .

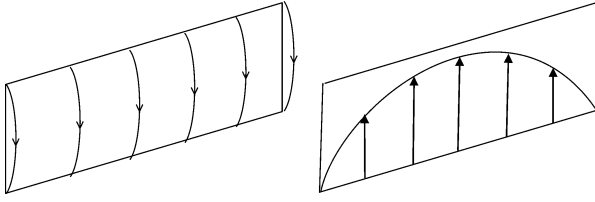


Fig. 3. Aperture electric fields of the folded horn, showing a slight nonplanarity (left) and showing a cosine-tapered magnitude variation (right).

The folded horn works as follows. The antenna is driven by an SMA connector that is positioned at the focus of the parabolic bend. Waves in the feed section expand in the H-plane until they reach the parabolic bend. After reflecting off the parabolic bend, the waves are focused in both E- and H-planes. The waves then proceed into aperture section, in which the fields are expanded in the E-plane. The fields remain focused in the H-plane, because of the parabolic bend. The fields in the E plane are only slightly out of focus, because there is little difference in ray path length between the central and extreme rays.

A sketch of the aperture electric fields appears in Fig. 3. On the left, we see that the electric fields protrude only slightly from the aperture, due to a slight defocus in the E-plane. On the right, we observe that the electric field magnitude varies approximately as a cosine function across the aperture, because of the metal walls on either side.

We begin the analysis by calculating the level of defocus in the aperture fields. We do so by calculating the path length difference between a central ray and an extreme ray in an E-plane cut through the Aperture Section, which has a length of  $3/4\lambda$ . We find the extreme ray has a length of  $0.79\lambda$ , compared to a direct path length down the center of  $0.75\lambda$ , resulting in a path length difference of  $0.04\lambda$ . So the aperture is essentially in focus.

Next, we calculate the boresight gain of such an aperture field distribution, assuming a focused aperture of size  $0.5 \times 2\lambda$ . We use the standard formula

$$G = e \frac{4\pi}{\lambda^2} A \quad (1)$$

where  $A$  is the aperture area,  $\lambda$  is the wavelength, and  $e$  is the aperture efficiency. Because of the cosinusoidal field distribution,  $e = 8/\pi^2 = 0.81$ , according to [1]. For this aperture,  $A = \lambda^2$ , so we have  $G = 32/\pi = 10.2 = 10.1$  dBi at the design frequency.

If one assumes a focused aperture, then the fields are similar to those of an open-ended waveguide (OEWG) [2, pp. 290–291]. In this case, the pattern functions are described by

$$F_H(\theta) = \frac{1 + \cos(\theta)}{2} \frac{\cos\left[\frac{\beta a}{2} \sin(\theta)\right]}{1 - \left[\frac{2}{\pi} \frac{\beta a}{2} \sin(\theta)\right]^2}$$

$$F_E(\theta) = \frac{1 + \cos(\theta)}{2} \frac{\sin\left[\frac{\beta b}{2} \sin(\theta)\right]}{\frac{\beta b}{2} \sin(\theta)} \quad (2)$$

where the long and short aperture dimensions are  $a$  and  $b$ , respectively,  $\beta = 2\pi/\lambda$ , and  $\theta$  is the angle from boresight. We plot these pattern functions later in the paper, next to our experimental data. A more accurate formulation would take into account the defocusing in the E-plane, using the expressions for the E-plane sectoral horn [2, pp. 306–310]. This has the same H-plane expression, but a different E-plane expression, which may be useful for larger E-plane opening angles.

### III. FOLDED HORN DESCRIPTION

We now provide the details of our folded horn, model FH-1E. A sketch of the configuration was shown earlier in Fig. 1, and photos are shown in Figs. 2 and 4. This antenna is designed to operate at 3 GHz, or

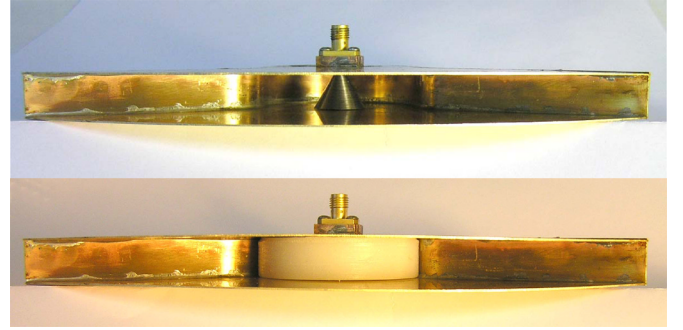


Fig. 4. Feed point detail of the FH-1E, before (top) and after (bottom) adding the dielectric disk.

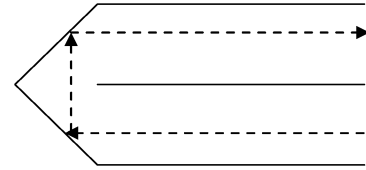


Fig. 5. Detail of the 180° bend, showing a typical ray path.

a wavelength of  $\lambda = 0.1$  m. Thus, the aperture is  $0.05 \times 0.2$  m ( $0.5 \times 2\lambda$ ), which makes the antenna small enough to allow easy construction and testing. The FH-1E was designed so it could be constructed entirely from flat pieces of sheet metal, with bends only in a single plane of curvature.

A number of features near the feed point require clarification. The feed point is located at the center of a cylinder, which is also the apex of the parabolic bend and the focus of the parabolic bend. The radius of the cylinder surrounding the feed point was chosen to be  $\lambda/4$  at the design frequency, 3 GHz in air. This was chosen so the short circuit at the edge of the cylinder would look like an open circuit at the feed.

We tried a number of different feed point designs before arriving at the final design, shown in Figs. 1 and 4. The feed point initially consisted of simply extending the center pin of the SMA connector all the way through the cavity, with a solder connection to the other side. In this configuration, we found that the antenna worked best near 5 GHz, which was well above our target frequency of 3 GHz. To reduce the operating frequency, we increased the electrical size of the disc by filling it with a dielectric material (Teflon,  $\epsilon_r = 2.1$ ). However, this still left us with an impedance spike at the feed point, as was apparent from TDR measurements. Thus, we replaced the straight pin with a cone embedded within the dielectric disc. The impedance of the cone was  $\sim 50 \Omega$  in the presence of the dielectric, using the standard expression for a cone above a ground plane. Details of the evolution of the feed point, including data obtained at intermediate steps, are provided in [3].

The shape of the parabolic bend also requires some clarification. The height of the feed section was  $\lambda/8$ , and it was desirable to keep the entire feed section within the  $\lambda/2$  height of the aperture. To conserve space, the bend was implemented as an abrupt 180° bend, using two 45° reflectors, as shown in Fig. 5. The dotted arrows show the path of a typical ray. With this configuration, all rays have the same path length around the bend, which keeps the wavefront in focus.

### IV. DATA

We characterized the antenna on our PATAR time domain antenna range. The source for this system is a Picosecond Pulse Labs Model 4015C step generator, which drives a Farr Research Model TEM-1-50 sensor. The 4015C is a high-speed pulser with a negative 4 V voltage step, with a fall time of 20 ps. The antenna under test was placed 4

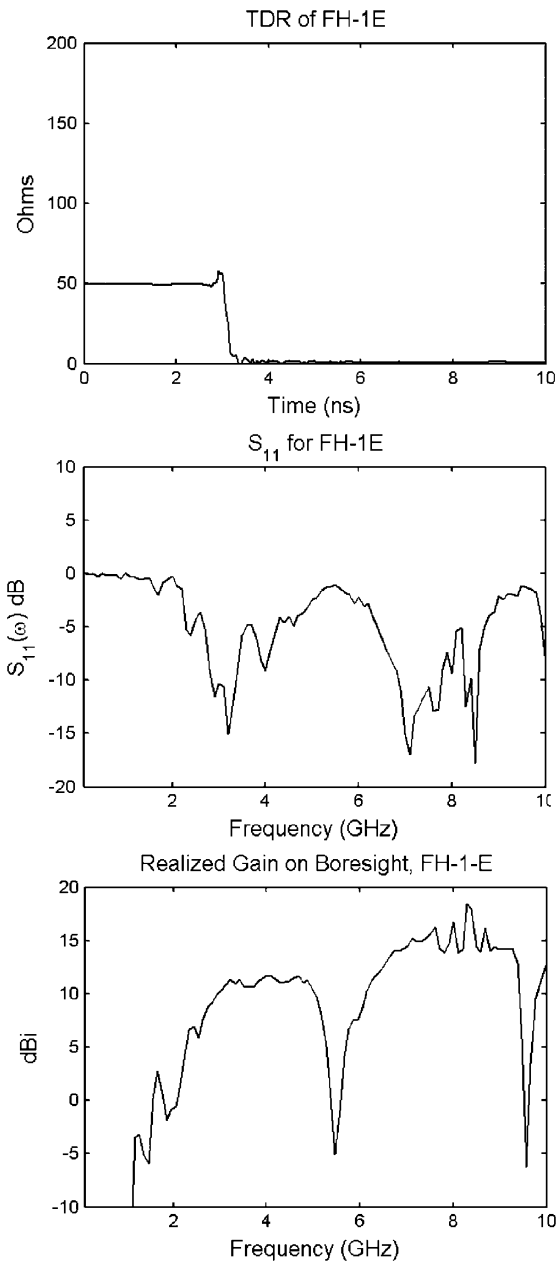


Fig. 6. TDR,  $S_{11}$ , and realized gain on boresight for the FH-1E.

m from the aperture of the TEM sensor. The output of the AUT was recorded using a Tektronix Model TDS8000 sampling oscilloscope, with a Model 80E04 sampling head.

In Fig. 6 we provide the TDR,  $S_{11}$ , and boresight realized gain of the FH-1E. Recall that realized gain is the gain reduced by return loss. The TDR at the feed point tapers smoothly from 50 to 0 ohms, as it should. The  $S_{11}$  has a dip near 3 GHz, the intended operating frequency. The realized gain is  $\geq 10$  dBi over a frequency range of 3–5 GHz, which is consistent with our earlier predictions at 3 GHz. The frequency range over which the return loss is  $-10$  dB or better is 2.8–3.35 GHz.

The antenna patterns in the H- and E-planes are shown in Fig. 7 at 3, 4, and 5 GHz. Alongside these, we plot the theoretical patterns of an OEWG with similar aperture dimensions. We see that the H-plane pattern is much narrower than the E-plane pattern, which we expect because of the aperture shape. The measured patterns are quite similar to the theoretical predictions, however, we observe

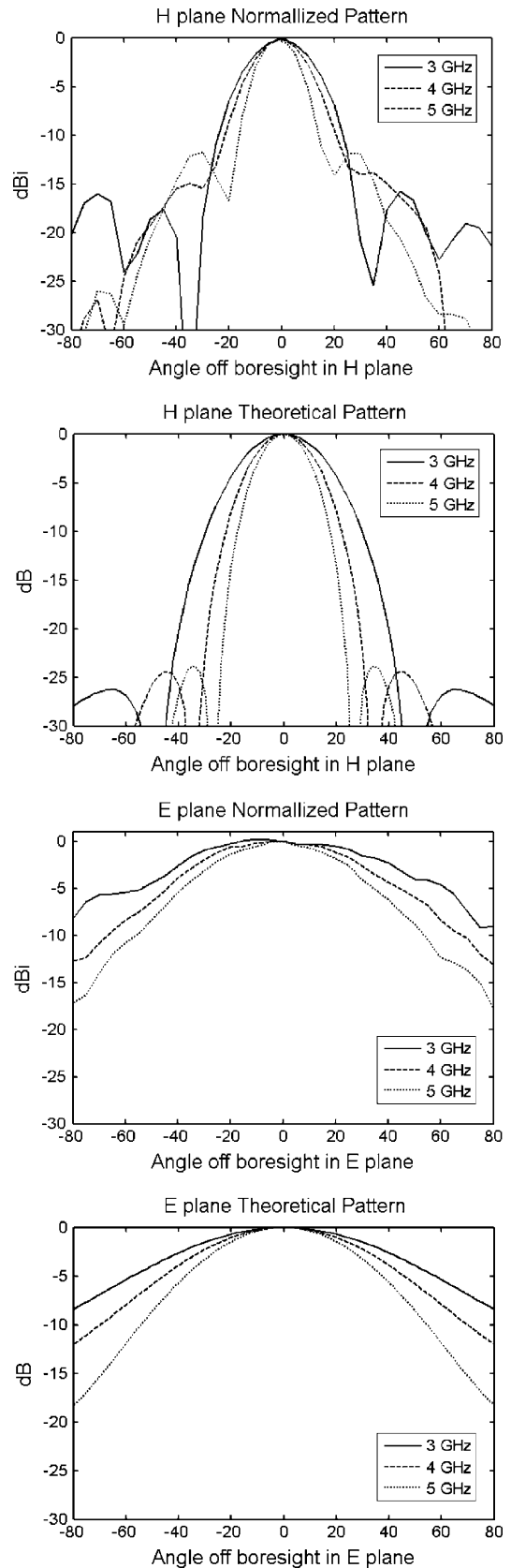


Fig. 7. Antenna patterns for the FH-1E in the H-plane (top) and E-plane (bottom) at 3, 4, and 5 GHz. Both experimental data and theoretical predictions are shown.

higher H-plane sidelobe levels in our experimental data than in the OEWG theory.

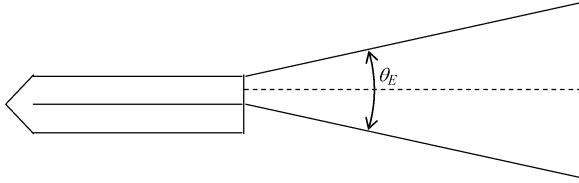


Fig. 8. Adjustment of the opening angle in the E-plane to optimize gain.

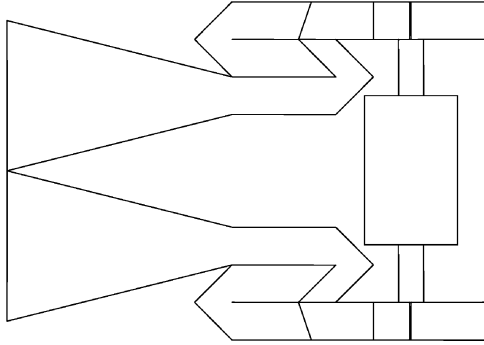


Fig. 9. Two bi-folded horns, positioned around a high-voltage source with differential output.

## V. IMPROVEMENTS TO THE FOLDED HORN

We summarize here the improvements to the folded horn that will be worth investigating in the future. First, it should be possible to further adjust the feed point to reduce the return loss over a broader frequency range. One might try varying the radius of the cylinder, the angle of the feed cone, and the dielectric constant of the disk.

Second, one might investigate the effect of the opening angle of the antenna in the E-plane,  $\theta_E$ , as shown in Fig. 8. We have configured the aperture height to be  $\lambda/2$ , but a larger aperture height and larger  $\theta_E$  might provide even more gain, with little disturbance to the focus in the E-plane. The current version has a difference in path length of just  $0.04\lambda$ , but it could probably tolerate the larger value that would come with a larger  $\theta_E$ .

Third, one could imagine a two-element array of folded horns stacked in the E-plane, in order to increase the aperture size. Such a device could be driven with a differential source, with equal-but-opposite output voltages. One might consider stacking two antennas similar to the FH-1E, but there might not be sufficient space between the two antennas for the high-power mesoband source. A better idea might be to use two bi-folded horns, as shown in Fig. 9. In this case, each of the bi-folded horns has, beginning at the feed point, an expansion section in the H-plane, a parabolic bend, a straight section, a straight bend, and an expansion section in the E-plane.

Finally, when adapting the design to higher voltages, three modifications may be useful. First, the Teflon cylindrical disk will be replaced with oil. Second, one might place a sharpening switch at the apex of the cone in the feed section. (In its simplest form, this is nothing more than a gap in the center conductor.) A sharpening switch would be challenging to implement in a dual configuration, because both switches would have to fire simultaneously, with low jitter. Finally, one might want to soften the  $180^\circ$  bend in the parabolic reflector, as shown in Fig. 10. Having a sharp knife-edge as shown in the left might induce flashover. Note that building rounded edges on a parabolic curve might be challenging. As an alternative, one might simply shorten the center conductor slightly, to remove the sharp edge from the region of high electric fields.

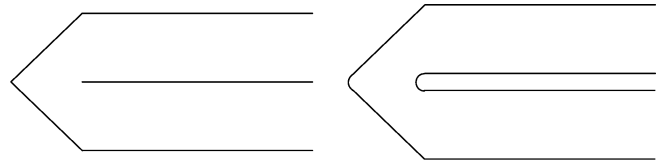


Fig. 10. Softening the  $180^\circ$  bend, current design (left) and proposed modification (right).

## VI. CONCLUSION

We have built and tested a folded horn, which is a compact antenna with moderate gain. After a number of iterations, we achieved a realized gain of 10 dBi or greater over a frequency range of 3–5 GHz. This was quite close to our predictions at 3 GHz, and it might be considered to be quite good performance for such a small antenna. The return loss was below  $-10$  dB over a frequency range of 2.8–3.35 GHz. The measured antenna pattern was quite close to that of an OEWG, except that the experimental data had higher H-plane sidelobe levels than predicted by the theory.

A number of areas are worth investigating to improve the folded horn, as described in Section V. These include investigations on refining the feed point, increasing the E-plane opening angle, and softening the  $180^\circ$  bend. Two antennas may be arrayed in the E-plane, each with either a single- or bi-folded design. The bi-folded design may be necessary to allow space for the source.

## ACKNOWLEDGMENT

The authors wish to thank the reviewers for their thoughts on improving the manuscript.

## REFERENCES

- [1] C. E. Baum, More Antennas for the Switched Oscillator Aug. 2004, Sensor and Simulation Note 493.
- [2] W. L. Stutzman and G. A. Thiele, *Antenna Theory and Design*, 2nd ed. New York: Wiley, 1998.
- [3] E. G. Farr, L. H. Bowen, C. E. Baum, and W. D. Prather, The Folded Horn Antenna Dec. 2006 [Online]. Available: [www.Farr-Research.com](http://www.Farr-Research.com), Sensor and Simulation Note 520